Ecological Indicators 117 (2020) 106545

Contents lists available at ScienceDirect

Ecological Indicators

journal homepage: www.elsevier.com/locate/ecolind

Applying Geodetector to disentangle the contributions of natural and anthropogenic factors to NDVI variations in the middle reaches of the Heihe River Basin

Lijun Zhu[a], Jijun Meng[a,*], Likai Zhu[b,*]

[a] Key Laboratory of Earth Surface Processes of Ministry of Education, College of Urban and Environmental Sciences, Peking University, Beijing 100871, China
[b] Shandong Provincial Key Laboratory of Water and Soil Conservation and Environmental Protection, College of Resources and Environment, Linyi University, Linyi, Shandong 276000, China

ARTICLE INFO

Keywords:
NDVI variations
Natural factors
Anthropogenic factors
Geodetector
The middle reaches of the Heihe River Basin

ABSTRACT

The detection and attribution of vegetation changes is a prerequisite for vegetation restoration and management. In arid and semi-arid areas, natural and anthropogenic factors interact to influence vegetation change, making it challenging to disentangle the contributions of driving forces. Here we used NDVI as an indicator of vegetation condition and analyzed its spatial and temporal changes in the middle reaches of the Heihe River Basin from 2000 to 2015. Then we applied the Geodetector method, a robust spatial statistics approach, to quantify the effects of natural and anthropogenic factors on NDVI changes. NDVI across the study area showed a significant increasing trend from 2000 to 2015. Both natural and anthropogenic factors were identified as significant driving forces of NDVI change, and the factors, land use conversion type, mean annual precipitation and soil type, caused the greatest influence. The explanatory power of a single factor was often enhanced when it interacted with other factors. We also found that influencing factors often correlated with NDVI changes in a nonlinear way. Our research highlights that the Geodetector method is an effective way to disentangle the complicated driving factors of vegetation change, and our results is useful for projecting vegetation change under future environmental change and taking measures to prevent and mitigate land degradation in drylands.

1. Introduction

Drylands cover about 41% of the Earth's land surface and support > 38% of the global population (Reynolds et al., 2007). Climate change and human activities have caused serious land degradation (e.g., desertification) in these areas (Reynolds et al., 2007), which in turn impedes social and economic development and threatens ecological environment. Monitoring land degradation and figuring out its potential causes is particularly important for sustainable land use. Vegetation is an important component of terrestrial ecosystems which links among the atmosphere, soil, water and other elements, and in drylands, it plays a particularly crucial role in providing ecosystem goods and services such as soil and water conservation, climate regulation, carbon and nitrogen cycling (Piao et al., 2011). Therefore, vegetation change can be a sensitive indicator of land degradation and ecosystem health (Casermeiro et al., 2004), and understanding its underlying driving mechanisms is prerequisite to develop effective strategies of vegetation restoration and desertification prevention.

The influencing mechanisms of vegetation change has been attracted much attention. Vegetation change has been found to be influenced by intertwined natural and anthropogenic factors. Natural factors mainly include atmospheric CO_2 concentrations, climate change (temperature, precipitation and radiation), and nitrogen deposition rate (Donohue et al., 2013; Los, 2013; Mao et al., 2013; Piao et al., 2015; Zhu et al., 2016b). Anthropogenic factors mainly include urbanization, agricultural fertilization and irrigation, grazing, deforestation, ecological restoration, and so forth (Mueller et al., 2014; Hua et al., 2017; Zhang et al., 2018). Given that the influences of these factors on vegetation changes are nonlinear and interacted, quantifying their contributions is challenging. Traditional statistical methods such as correlation and regression is effective only when the relationships between vegetation change and its driving forces are linear (Gu et al., 2018), and dependent and independent variables follow normal distributions. But in reality, these conditions are rarely satisfied. For example, the responses of vegetation NPP to precipitation vary with amount, seasonality and frequency (Gerten et al., 2008; Peng et al., 2013), and the

* Corresponding authors.
E-mail addresses: jijunm@pku.edu.cn (J. Meng), zhulikai@lyu.edu.cn (L. Zhu).

https://doi.org/10.1016/j.ecolind.2020.106545
Received 30 January 2020; Received in revised form 3 May 2020; Accepted 15 May 2020

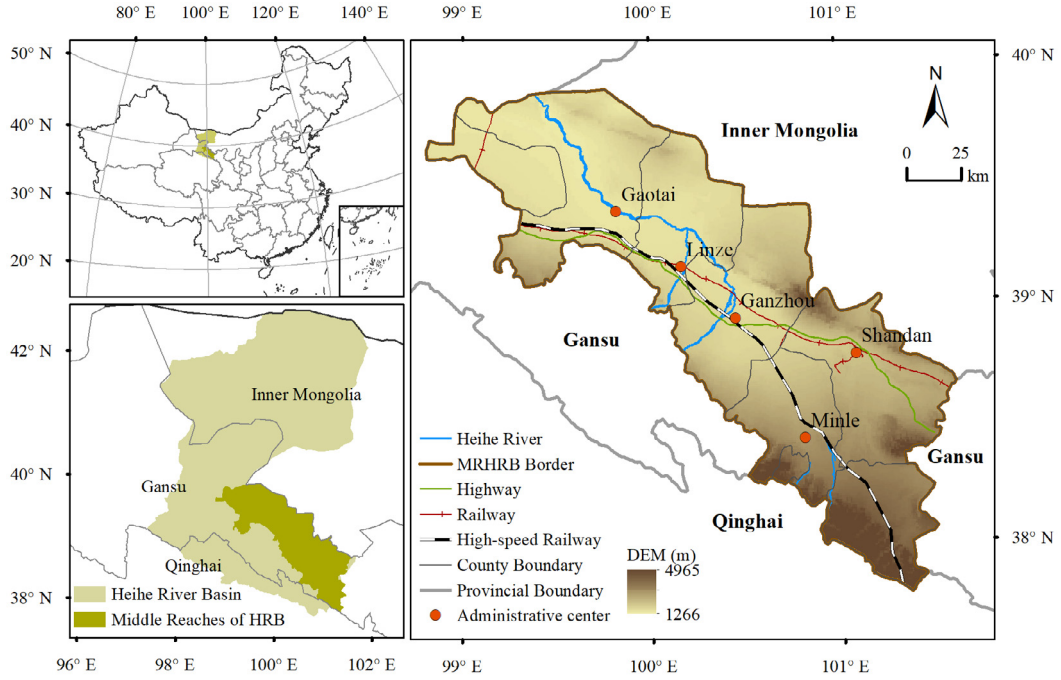

Fig. 1. The location of the study area.

relationship between vegetation photosynthesis and temperature has been proved to be non-linear (Yamori et al., 2014). The nonlinearity is often influenced by the changes in other factors as indicated by the weakening relationship between temperature and vegetation activity over time, due to more severe drought in the temperate ecosystems, increase in extremely hot days and shrub expansion over grass-dominated tundra in the arctic ecosystems (Piao et al., 2014). Dynamic ecosystem models allow the response of environmental variables to key processes (such as photosynthesis, respiration, evapotranspiration, phenology, and carbon allocation) to be analyzed in a nonlinear and dynamic way (Oleson et al., 2010; Piao et al., 2015), overcoming the limitations of traditional statistical method (Peng et al., 2013; Piao et al., 2014). However, ecosystem models usually require to set a large number of model parameters, which potentially causes much more uncertainties (Sitch et al., 2008). In contrast, Geodetector is a robust and straightforward method to quantify the influences of driving factors and their interactions (Wang and Xu, 2017), which does not have to follow restrictedly the assumptions of traditional statistical methods, and involve complex processes of parameter settings. Thus, this method has been successfully used to quantify the effects of driving factors on the vegetation change (Liang and Yang, 2016; Pan et al., 2019; Peng et al., 2019; Zhang and Zang, 2019), and will potentially be an effective tool to disentangle the causes of vegetation change in dryland ecosystems.

The influence of anthropogenic factors on vegetation growth is much more difficult to quantify than natural drivers. Human-induced land degradation has been detected by analyzing the trend of residues which are calculated as the differences between the actual NDVI value and the estimated NDVI value fitted with only natural factors as independent variables (A et al., 2016). However, this method has a limited range conditions within which they are reliable indicators of land degradation (Wessels et al., 2012). For example, land degradation can only be effectively detected when there is a 30–40% reduction in the sum of NDVI ($\sum NDVI$), given the underlying positive trend in $\sum NDVI$ caused by increased rainfall. Land use involves the management and modification of natural environment or wilderness into built environment such as settlements and semi-natural habitats such as arable fields, pastures, and managed woods, thus land use change is considered to be the most direct and comprehensive indicator of human activities (Zhang and Zang, 2019). Land use change has been proved to be the main driving factor of long-term changes in vegetation in China (Hua et al., 2017; Piao et al., 2019). Urbanization, characterized by the occupation of croplands, forests and grasslands by impervious surface, has removed vegetation or change vegetation structure in urban areas (Qu et al., 2020). Irrigation and fertilization promote crop growth in agricultural areas (You et al., 2019). Afforestation, benefited from ecological protection policies, for example, the Grain for Green Project, has contributed a lot to vegetation improvement (Qu et al., 2020). Therefore, exploring the relationship between land use change and vegetation change can effectively reveal the influence of human activities on vegetation growth.

China is one of the countries severely affected by desertification, especially in the agro-pastoral transitional zone in northern China and the oases along inland rivers in the arid areas of northwestern China (Wu and Ci, 2002). The Heihe River is the second largest inland river in China, located in the typical arid and semi-arid regions in northwestern China. Its eco-environment is extremely fragile and sensitive (Wang and Pan, 2019). The middle reaches of the Heihe River Basin are characterized by the most intensive human activities, the most densely distributed oases, and the most developed economy across the whole Heihe River Basin. Vegetation is an essential element for sustainable development and ecological security. Therefore, the middle reach of the Heihe River Basin is an ideal place to study the vegetation variations and their responses to natural factors and human activities in the arid and semi-arid areas. Studies have found that precipitation has the greatest impact on vegetation change in the middle reaches of the Heihe River among natural factors, and then was followed by soil type (Fu et al., 2018; Yuan et al., 2019). Human activities were rarely considered, and the interactions between factors and the non-linearity of the influence of factors are often not addressed effectively. Therefore, our archiving goal is to disentangle the contributions of natural and anthropogenic factors to vegetation changes in the middle reaches of the Heihe River Basin from 2000 to 2015. To achieve this goal, we first analyzed the temporal and spatial variations in NDVI, and then quantified how natural and anthropogenic factors interact to influence these changes using the robust Geodetector method.

Table 1
Classes of annual maximum NDVI change.

Significance level	Slope	Classes
$p < 0.05$	slope ≥ 0.01	Significant improvement
	0 < slope < 0.01	Slight improvement
	−0.01 < slope ≤ 0	Slight degradation
	slope ≤ -0.01	Significant degradation
$p \geq 0.05$	slope > 0	Insignificant improvement
	slope ≤ 0	Insignificant degradation

2. Materials and methods

2.1. Study area

The Heihe River originates from the Qilian Mountains in Qinghai, flows through Gansu and disappears in oases in Inner Mongolia, and its basin is located in the transition zone between the Qinghai-Tibet Plateau and Inner Mongolia Plateau. The middle reaches of the Heihe River Basin (97°20′–102°12′E and 37°28′–39°57′N) (Fig. 1) is between Yingluo Gorge and Zhengyi Gorge, covering an area of 1.96×10^4 km^2. It is adjacent to Qilian Mountains in the south and to Longshou Mountains and Heli Mountains in the north, while plains are distributed in the middle. Across the study area, oases, deserts and Gobi are intermittently distributed. The altitude is high in the south and low in the north, ranging from 1266–4965 m. The study area belongs to a temperate continental arid climate with an annual precipitation of 100–676 mm decreasing from south to north and from east to west, and annual temperatures of −7–10 °C increasing from south to north and from east to west. Unused land accounts for approximately 50% of the total area, mainly distributed in the northwest; cultivated land accounts for about 20%, mainly in the central corridor plains; and forests and grasslands are mainly in the south. The administrative units of our study area include Ganzhou, Linze, Minle, Shandan, Gaotai and Minghua in Zhangye City, Gansu Province.

2.2. Data sources

We collected data for vegetation conditions and their driving factors from multiple sources. We used the annual maximum NDVI as a dependent variable to analyze vegetation change and determine its underlying mechanisms. This dataset was derived from the continuous time series of SPOT VEGETATION NDVI through maximum value composite method, and was free downloaded from the Resource and Environment Data Cloud Platform, Chinese Academy of Sciences (http://www.resdc.cn) at a 1-km resolution from 2000 to 2015 (Xu, 2018). It has been widely used, and proven to be effective in reflecting vegetation coverage and change in China (Chen et al., 2020). Gridded climate data used in our research included annual precipitation and temperature data with a 1 km resolution from 2000 to 2015. They were generated through spatial interpolation based on daily data of national meteorological stations, and could be downloaded from the Resource and Environment Data Cloud Platform, Chinese Academy of Sciences (http://www.resdc.cn). We used DEM data with a 1 km resolution to extract elevation, slope and aspect across our study area. We use land cover maps in 2000 and 2015 to generate the independent variable of land use conversion. The data set was interpreted visually based on Landsat TM/ETM + images of various periods, and available from the multi-temporal land use database of China. We reclassified land cover types into 6 types: cropland, forest, grassland, water area, construction land and unused land, and generated a map of land use conversion between 2000 and 2015. Spatial distribution of landform type with a 1 km resolution was collected from the Cold and Arid Regions Science Data Center (http://westdc.westgis.ac.cn/). The data of basic geographic information data, including cities, roads, rivers, and so forth, were collected from the National Geomatics Center of China (http://www.ngcc.cn/ngcc/).

2.3. Methods

2.3.1. Trend analysis of NDVI

Annual maximum NDVI can effectively reflect annual vegetation growth conditions, and is widely used to analyze vegetation dynamics (Peng et al., 2019). We used the linear regression method to detect the trend of annual maximum NDVI of the study area as a whole and by pixel from 2000 to 2015. The slope of linear regression can reflect the change rate of annual maximum NDVI which can be estimated as:

$$\text{slope} = \frac{n \times \sum_{j=1}^{n} (j \times \text{NDVI}_j) - \sum_{j=1}^{n} j \sum_{j=1}^{n} \text{NDVI}_j}{n \times \sum_{j=1}^{n} j^2 - (\sum_{j=1}^{n} j)^2} \quad (1)$$

where n is the number of years, and NDVI_j is annual maximum NDVI of year j. We classified NDVI changes into 6 classes according to the slope and the significance level (Table 1) (Liu et al., 2016).

2.3.2. Factors selection

Complex and diverse environmental variables and human activities influence the change of NDVI (Piao et al., 2015; Ma et al., 2019). We chose NDVI change value between 2000 and 2015 as the dependent variable which was defined as the NDVI value in 2015 minus the NDVI value in 2000 and selected 10 natural and anthropogenic factors from the respects of climate, topography, geomorphology, soil, river and human activity, which were representative and easy to quantify, and whose data are readily available (Table 2). Precipitation and temperature are two of the most important influencing factors of vegetation changes (Gu et al., 2018; Yuan et al., 2019). Although some environmental elements such as elevation, slope, aspect, landform type and soil type change slightly in a short period, they provide very important environmental context for vegetation changes (Zhang et al., 2018; Peng et al., 2019). Beyond precipitation, rivers are the main water sources to support vegetation growth in the arid areas, so we included the distance to the rivers as one independent variable (Liang and Yang, 2016). Studies have proven that the distance to the urban centers and land use conversion types can effectively reflect the magnitude of human influences, so we have included these two factors as independent variables (Liu and Li, 2017).

Given that the Geodetector method was only able to deal with discrete variables (Wang and Xu, 2017), we converted the 10 continuous variables into discrete ones (Table 3). The natural breaks method built in ArcGIS determines the clustering according to the inherent attribute of data in order to reduce the variance within the group and increase the variance between the groups, which has been widely used in data classification when applying the Geodetector method (Liu and Li, 2017; Peng et al, 2019). It was used to divide mean annual precipitation, mean annual temperature and elevation into 6 discrete grades and divide slope into 10 grades. Aspect was classified into 9 types according to relevant studies (Zhang et al., 2017; Peng et al., 2019). Landform had 6 types: plains, platforms, hills, small undulating

Table 2
Potential natural and anthropogenic factors of vegetation change.

Respects	Variables	Code	Unit
Climate	Mean annual precipitation	x_1	mm
	Mean annual temperature	x_2	°C
Topography	Elevation	x_3	m
	Slope	x_4	°
	Aspect	x_5	°
Geomorphology	Landform type	x_6	categorical
Soil	Soil type	x_7	categorical
River	Distance to the rivers	x_8	km
Human activity	Distance to the urban centers	x_9	km
	Land use conversion type	x_{10}	categorical

Table 3
Factors grading standards.

Categories \Factors	Mean annual precipitation (mm)	Mean annual temperature (°C)	Elevation (m)	Slope (°)	Aspect (°)	Landform type	Soil type	Distance to the rivers (km)	Distance to the urban centers (km)
1	100.46–173.54	−6.85 to −0.25	1256–1571	0–0.74	Gentle slope (−1°)	Plains	Semi-leached soils	0–3	0–3
2	173.54–242.84	−0.25–2.83	1571–1905	0.74–1.55	North slope (0–22.5°, 337.5–360°)	Platforms	Calcic soils	3–10	3–8
3	242.84–320.71	2.83–5.14	1905–2320	1.55–2.59	Northeast slope (22.5–67.5°)	Hills	Arid soils	10–20	8–15
4	320.71–406.42	5.14–7.04	2320–2791	2.59–3.98	East slope (67.5–112.5°)	Small undulating mountains	Desert soils	20–30	15–25
5	406.42–509.96	7.04–8.48	2791–3393	3.98–5.84	Southeast slope (112.5–157.5°)	Medium undulating mountains	Primary soils	30–50	25–35
6	509.96–675.40	8.48–9.61	3393–4685	5.84–8.13	South slope (157.5–202.5°)	Large undulating mountains	Semi-hydromorphic soils	50–91	35–56
7				8.13–10.88	Southwest slope (202.5–247.5°)		Hydromorphic soils		
8				10.88–14.10	West slope (247.5–292.5°)		Saline-alkali soils		
9				14.10–18.24	Northwest slope (292.5–337.5°)		Anthropogenic soils		
10				18.24–27.58			Alpine soils		
11							Lakes and reservoirs		
12							Rivers		
13							Glaciers		

mountains, medium undulating mountains and large undulating mountains. Soil included 13 categories based on soil order: semi-leached soil, calcic soil, arid soil, desert soil, primary soil, semi-hydromorphic soil, hydromorphic soil, saline-alkali soil, anthropogenic soil, alpine soil, lakes and reservoirs, rivers, and glaciers. Distances to the rivers and to the urban centers were divided into 6 grades by the natural breaks method. There were 28 types of land use conversion as shown in Fig. 2(j). We showed the spatial distribution of grades for all factors (Fig. 2), and summarized the average NDVI within each grade of a specific factor to initially illustrate their relationships (Fig. 3).

2.3.3. *Geodetector*

We used the Excel Geodetector software which was developed by Wang et al. (2010) to implement the Geodetector method. The software can be downloaded free of charge from the website (http://www.geodetector.cn/). The Geodetector method was used to detect the influence of our selected 10 factors on vegetation changes. It is a spatial statistics method to detect spatial heterogeneity and quantify the influence of driving factors. Geodetector is not based on linear assumptions, but compares the spatial consistency of independent variable distribution versus the geographical strata in which potential factors exist. The basic principle is to divide the total sample into several subsamples and judge the spatial heterogeneity and variable relationships by variance. If the sum of the variances of subsamples is less than the total variance of all samples, spatial differences exist. If the spatial distributions of two variables tend to be consistent, there is a statistical correlation between these two variables (Wang and Xu, 2017). Geodetector includes 4 aspects of detection (Wang et al., 2010).

(1) Factor detector. Factor detector identifies factors that are responsible for the independent variable. The explanatory power of each factor is measured by q value:

$$q=1-\frac{\sum_{h=1}^{L} N_h \sigma_h{}^2}{N\sigma^2} \tag{2}$$

where q is the explanatory power of one factor on vegetation NDVI change; h is the number of classifications or partitions of Y or factor X; N_h and N are the number of units in class h and the whole region, respectively; $\sigma_h{}^2$ and σ^2 are the variance of Y for the units in class h and the whole region, respectively. The q value ranges from 0 to 1, and the larger the q value is, the stronger the spatial heterogeneity of Y is. If h is generated by factor X , the q value indicates that X explains $100 \times q$% of Y. The larger the q value is, the stronger the explanatory power of factor X to Y is, and vice versa. The q value followed the Noncentral F-test (Wang et al., 2016) which was used to determine the significance level.

(2) Ecological detector. Ecological detector determines whether there is a significant difference between two factors (X_1 and X_2) in terms of their influence on the spatial pattern of NDVI change, which is examined by F statistic:

$$F=\frac{N_{X_1}(N_{X_2}\text{-}1)\,\mathrm{SSW}_{X_1}}{N_{X_2}(N_{X_1}\text{-}1)\,\mathrm{SSW}_{X_2}} \tag{3}$$

$$\mathrm{SSW}_{X_1}=\frac{\sum_{h=1}^{L_1} N_h \sigma_h{}^2}{N\sigma^2},\ \mathrm{SSW}_{X_2}=\frac{\sum_{h=1}^{L_2} N_h \sigma_h{}^2}{N\sigma^2} \tag{4}$$

where N_{X_1} and N_{X_2} represent the sample number of two factors (X_1 and X_2), respectively. SSW_{X_1} and SSW_{X_2} represent the sum of variance of each class formed by two factors (X_1 and X_2), respectively. L_1 and L_2 represent the number of classes for variable X_1 and X_2, respectively. F-test was used to determine the significance level of F statistic.

(3) Risk detector. Risk detector judges whether there is a significant difference between mean values of Y in two subzones of a factor,

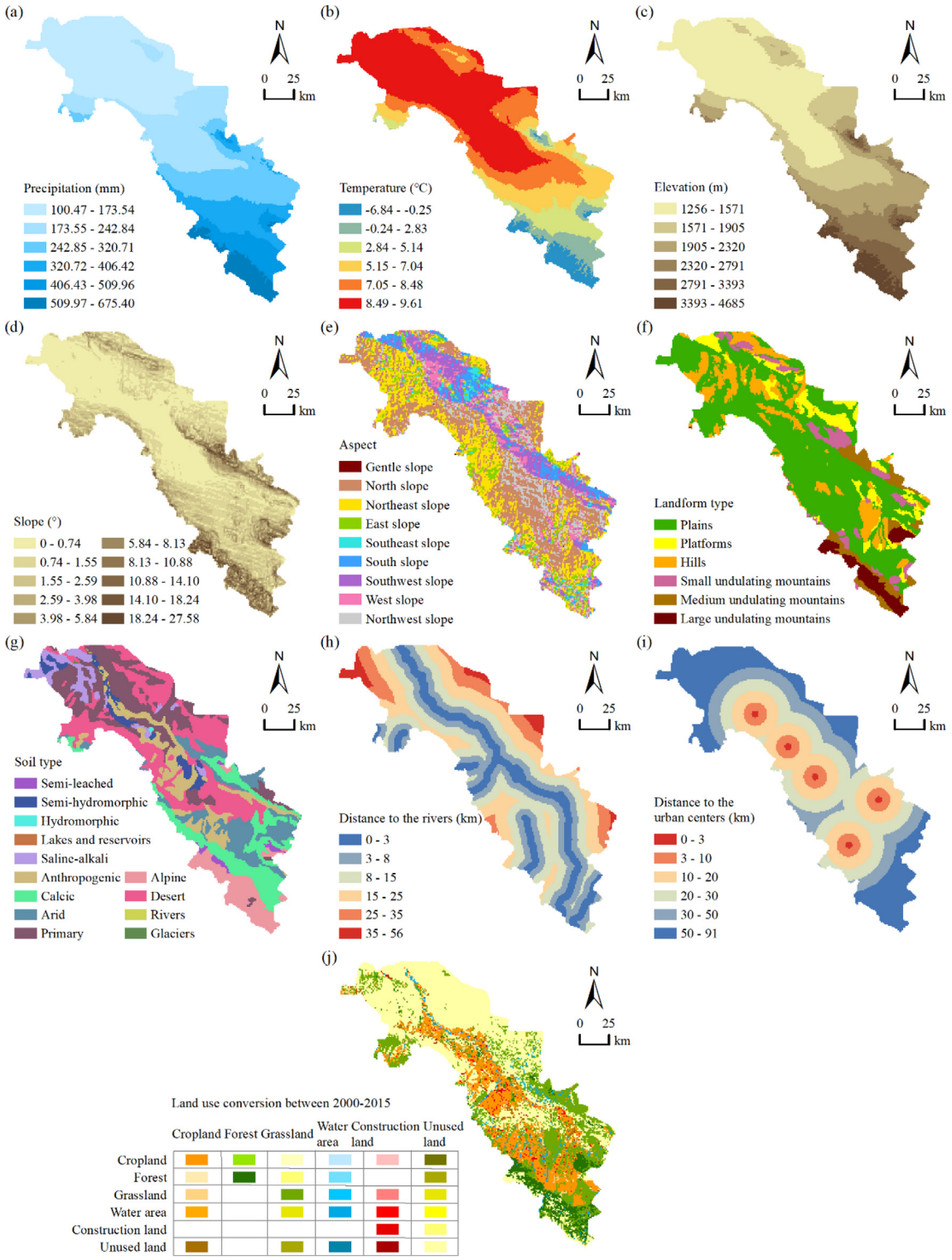

Fig. 2. The spatial distributions of all factors in study area.

which is examined by t statistic:

$$t = \frac{\overline{Y}_{h=1} - \overline{Y}_{h=2}}{\left[\frac{Var(\overline{Y}_{h=1})}{n_{h=1}} + \frac{Var(\overline{Y}_{h=2})}{n_{h=2}}\right]^{1/2}} \quad (5)$$

where $\overline{Y}_h$ represents the mean value of attributes in the sub-region h, n_h is the number of samples in the sub-region h, and Var represents the variance. The t value follows the Student's t test, which can test whether the influence of natural or anthropogenic factor is statistically significant or not at specific significance level.

(4) Interaction detector. Interaction detector assesses whether the explanatory powers of two factors are enhanced, weakened, or independent of each other. First, the q values of two factors X_1 and X_2 for Y were calculated ($q(X_1)$ and $q(X_2)$). Then, the q value of interaction, which is a new layer formed by tangent of overlay variables X_1 and X_2, was calculated ($q(X_1 \cap X_2)$) and compared with $q(X_1)$ and $q(X_2)$ to indicate the interaction type between two

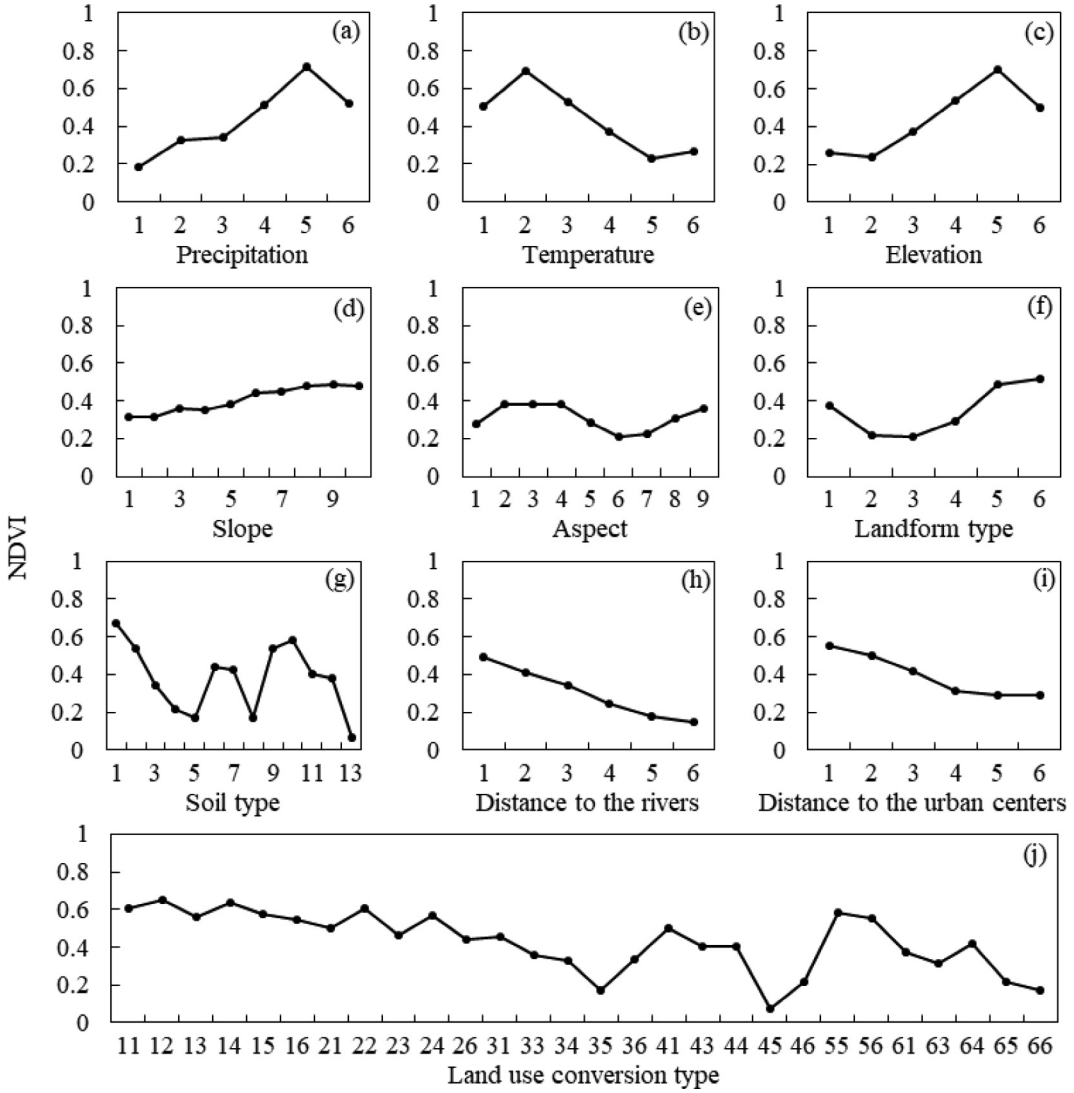

Fig. 3. The variations in the average NDVI values with different grades for all factors. The meanings of the codes for land use conversion type can be found in Fig. 2(j).

variables.

3. Results

3.1. Spatial and temporal pattern of NDVI change

Annual maximum NDVI of the whole study area showed an increasing trend at a rate of 0.0052/year (Fig. 4). The areas where NDVI changed significantly from 2000 to 2015 was 9757 km^2, accounting for 48.9% of the total area. The areas showing an increasing trend accounted for 48.4% of the total area, among which 15.7% increased significantly. In contrast only 0.46% of the total area showed a decreasing trend.

We used the NDVI data products generated by Xu et al. (2018), of which the NDVI values were normalized between 0 and 1. The distribution of mean annual maximum NDVI showed a clear spatial pattern. Vegetation NDVI was at a low level with mean annual maximum NDVI < 0.6 in most areas. The lowest NDVI values were mainly distributed in the northwest with average values < 0.10, where deserts and Gobi were mainly distributed (Fig. 5a). The highest NDVI values were mainly distributed in the oases along the Heihe River and southern Qilian mountains. The areas with significantly increased NDVI were mainly distributed along the Heihe River, and in the central and

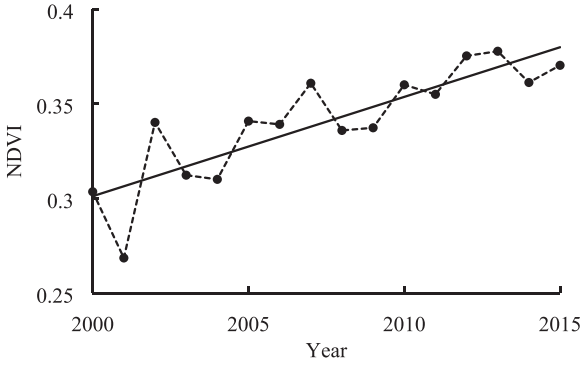

Fig. 4. Trend of annual maximum NDVI in the middle reaches of the Heihe River.

southern areas of our study area (Fig. 5b), which was consistent with findings of previous research (Wang et al., 2019; You et al., 2019). The oases along the rivers and in the central plains have witnessed flourished crops due to developed irrigation system and abundant water supply. The southern areas were mainly covered by forests and

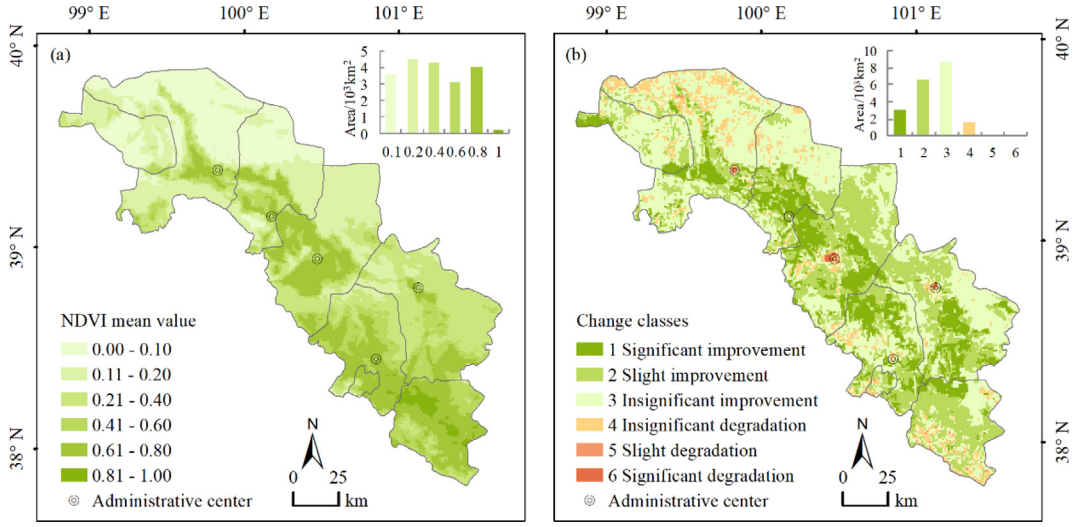

Fig. 5. Spatial pattern of mean annual maximum NDVI (a) and change classes (b) in the middle reaches of the Heihe River Basin.

grasslands whose conditions had been recovered due to increased precipitation and intensive management. The areas with significantly decreased NDVI were distributed sparsely around administrative centers, and areas with decreased NDVI but not significantly were distributed in upstream mountain areas and downstream plain areas. Urban expansion has occupied a large amount of farmlands and ecological lands, causing a decrease in NDVI. Research has found that climate change, especially temperature change, has the profound impacts on vegetation dynamics (Li et al., 2020). Warming climate might amplify climate variability, make extreme climate events occur more frequently (Liu et al, 2013), which leads to a decrease in vegetation productivity in upstream mountain areas. In contrast, anthropogenic factors (e.g., land use changes) are the dominant driving forces of vegetation dynamics in the downstream plain areas (Li et al., 2020). Although agriculture expansion and intensification leads to an increase in vegetation productivity, the problems of salinization and desertification are severe in these areas, which results in vegetation degradation.

3.2. Influence of natural and anthropogenic factors

All 10 factors exerted significant effect on NDVI changes ($p < 0.05$). The factor, land use conversion type, had the largest influence which explained 23.9% of NDVI changes. The following factors were mean annual precipitation and soil type, whose contributions were 15.8% and 11.6%, respectively. The factors, elevation, mean annual temperature, distance to the urban centers, distance to the rivers, aspect and landform type explained only 9.5%, 7.4%, 6.2%, 3.2%, 2.5%, and 1.6% respectively. The contribution of slope degree was the lowest (0.2%). Therefore, both natural and anthropogenic factors had been identified as important influencing factors of NDVI changes in our study area.

3.3. Significant differences between factors

Most pairs of factors showed a significant difference regarding their influences on NDVI changes except the pairs of mean annual temperature and distance to the urban centers, landform type and slope, landform type and aspect, landform type and distance to the rivers, and aspect and distance to the rivers (Table 4). We found that the factors, land use conversion type, mean annual precipitation and soil type, which had greater contributions, all had statistically significant differences with other factors. Therefore, the factors, land use conversion type, mean annual precipitation and soil type are key factors which influenced vegetation changes in their own ways in the middle reaches of Heihe River Basin.

Table 4
Ecological detector results showing whether the effects of the two factors on vegetation NDVI changes have a significant difference at a confidence level of 0.95.

Factors	x_1	x_2	x_3	x_4	x_5	x_6	x_7	x_8	x_9	x_{10}
x_1										
x_2	Y									
x_3	Y	Y								
x_4	Y	Y	Y							
x_5	Y	Y	Y	Y						
x_6	Y	Y	Y	N	N					
x_7	Y	Y	Y	Y	Y	Y				
x_8	Y	Y	Y	Y	N	N	Y			
x_9	Y	N	Y	Y	Y	Y	Y	Y		
x_{10}	Y	Y	Y	Y	Y	Y	Y	Y	Y	

Note: Y indicates that there is a significant difference in the effects of the two factors on vegetation NDVI changes, and N means no significant difference.

3.4. Interaction between factors

If the q statistics for factor interactions is greater than the maximum of both x_1 and x_2 but less than the sum of them (Max(A, B) < C < A + B), it indicates that the two factors are mutually enhanced. If the q statistics for factor interactions is even greater than the sum of x_1 and x_2 (C > A + B), it indicates that the two factors are non-linearly enhanced. The q statistics for factor interactions were higher than the q statistics for a single factor, indicating that the explanatory power of a single factor could be enhanced when interacting with others (Table 5). For 67% of cases, the q statistics for interaction between two factors were higher than the sum of the q statistics of two single factors, which suggested a non-linear enhancement effect.

3.5. Non-linear effects of factors

The risk detector results could reflect how NDVI change responded to changes in the level of a specific factor in a non-linear way. The results showed that NDVI varied non-linearly with the levels of all factors (Fig. 6a-i). For example, the influence of precipitation varied with the levels of precipitation, although NDVI increased consistently with precipitation (Fig. 6a). With an increase in precipitation, the magnitude of NDVI increase rose and reached the peak of 0.13 at level 5 (406–509 mm), and then decreased to the second minimum increasing

Table 5
Influence of the interaction between pairs of factors.

Max (A, B)	C	A + B	Results	Interpretation	Max (A, B)	C	A + B	Results	Interpretation
$x_1 = 0.158 <$	$x_1 \cap x_2 = 0.221$	$< 0.232 = x_1 + x_2$	C < A + B	↑	$x_{10} = 0.239 <$	$x_3 \cap x_{10} = 0.311$	$< 0.335 = x_3 + x_{10}$	C < A + B	↑
$x_1 = 0.158 <$	$x_1 \cap x_3 = 0.204$	$< 0.254 = x_1 + x_3$	C < A + B	↑	$x_5 = 0.025 <$	$x_4 \cap x_5 = 0.041$	$> 0.027 = x_4 + x_5$	C > A + B	↑↑
$x_1 = 0.158 <$	$x_1 \cap x_4 = 0.230$	$> 0.160 = x_1 + x_4$	C > A + B	↑↑	$x_6 = 0.016 <$	$x_4 \cap x_6 = 0.033$	$> 0.018 = x_4 + x_6$	C > A + B	↑↑
$x_1 = 0.158 <$	$x_1 \cap x_5 = 0.178$	$< 0.183 = x_1 + x_5$	C < A + B	↑	$x_7 = 0.116 <$	$x_4 \cap x_7 = 0.153$	$> 0.118 = x_4 + x_7$	C > A + B	↑↑
$x_1 = 0.158 <$	$x_1 \cap x_6 = 0.203$	$> 0.174 = x_1 + x_6$	C > A + B	↑↑	$x_8 = 0.032 <$	$x_4 \cap x_8 = 0.052$	$> 0.034 = x_4 + x_8$	C > A + B	↑↑
$x_1 = 0.158 <$	$x_1 \cap x_7 = 0.211$	$< 0.275 = x_1 + x_7$	C < A + B	↑	$x_9 = 0.062 <$	$x_4 \cap x_9 = 0.096$	$> 0.064 = x_4 + x_9$	C > A + B	↑↑
$x_1 = 0.158 <$	$x_1 \cap x_8 = 0.197$	$> 0.190 = x_1 + x_8$	C > A + B	↑↑	$x_{10} = 0.239 <$	$x_4 \cap x_{10} = 0.253$	$> 0.241 = x_4 + x_{10}$	C > A + B	↑↑
$x_1 = 0.158 <$	$x_1 \cap x_9 = 0.254$	$> 0.220 = x_1 + x_9$	C > A + B	↑↑	$x_5 = 0.025 <$	$x_5 \cap x_6 = 0.044$	$> 0.041 = x_5 + x_6$	C > A + B	↑↑
$x_{10} = 0.239 <$	$x_1 \cap x_{10} = 0.360$	$< 0.398 = x_1 + x_{10}$	C < A + B	↑	$x_7 = 0.116 <$	$x_5 \cap x_7 = 0.148$	$> 0.141 = x_5 + x_7$	C > A + B	↑↑
$x_3 = 0.095 <$	$x_2 \cap x_3 = 0.118$	$< 0.169 = x_2 + x_3$	C < A + B	↑	$x_8 = 0.032 <$	$x_5 \cap x_8 = 0.076$	$> 0.057 = x_5 + x_8$	C > A + B	↑↑
$x_2 = 0.074 <$	$x_2 \cap x_4 = 0.112$	$> 0.076 = x_2 + x_4$	C > A + B	↑↑	$x_9 = 0.062 <$	$x_5 \cap x_9 = 0.095$	$> 0.087 = x_5 + x_9$	C > A + B	↑↑
$x_2 = 0.074 <$	$x_2 \cap x_5 = 0.106$	$> 0.099 = x_2 + x_5$	C > A + B	↑↑	$x_{10} = 0.239 <$	$x_5 \cap x_{10} = 0.263$	$< 0.264 = x_5 + x_{10}$	C < A + B	↑
$x_2 = 0.074 <$	$x_2 \cap x_6 = 0.122$	$> 0.089 = x_2 + x_6$	C > A + B	↑↑	$x_7 = 0.116 <$	$x_6 \cap x_7 = 0.152$	$> 0.132 = x_6 + x_7$	C > A + B	↑↑
$x_7 = 0.116 <$	$x_2 \cap x_7 = 0.144$	$< 0.190 = x_2 + x_7$	C < A + B	↑	$x_8 = 0.032 <$	$x_6 \cap x_8 = 0.066$	$> 0.047 = x_6 + x_8$	C > A + B	↑↑
$x_2 = 0.074 <$	$x_2 \cap x_8 = 0.131$	$> 0.105 = x_2 + x_8$	C > A + B	↑↑	$x_9 = 0.062 <$	$x_6 \cap x_9 = 0.092$	$> 0.078 = x_6 + x_9$	C > A + B	↑↑
$x_2 = 0.074 <$	$x_2 \cap x_9 = 0.187$	$> 0.136 = x_2 + x_9$	C > A + B	↑↑	$x_{10} = 0.239 <$	$x_6 \cap x_{10} = 0.255$	$> 0.255 = x_6 + x_{10}$	C > A + B	↑↑
$x_{10} = 0.239 <$	$x_2 \cap x_{10} = 0.291$	$< 0.313 = x_2 + x_{10}$	C < A + B	↑	$x_7 = 0.116 <$	$x_7 \cap x_8 = 0.174$	$> 0.148 = x_7 + x_8$	C > A + B	↑↑
$x_3 = 0.095 <$	$x_3 \cap x_4 = 0.152$	$> 0.097 = x_3 + x_4$	C > A + B	↑↑	$x_7 = 0.116 <$	$x_7 \cap x_9 = 0.217$	$> 0.178 = x_7 + x_9$	C > A + B	↑↑
$x_3 = 0.095 <$	$x_3 \cap x_5 = 0.123$	$> 0.120 = x_3 + x_5$	C > A + B	↑↑	$x_{10} = 0.239 <$	$x_7 \cap x_{10} = 0.327$	$< 0.356 = x_7 + x_{10}$	C < A + B	↑
$x_3 = 0.095 <$	$x_3 \cap x_6 = 0.144$	$> 0.111 = x_3 + x_6$	C > A + B	↑↑	$x_9 = 0.062 <$	$x_8 \cap x_9 = 0.087$	$< 0.094 = x_8 + x_9$	C < A + B	↑
$x_7 = 0.116 <$	$x_3 \cap x_7 = 0.141$	$< 0.212 = x_3 + x_7$	C < A + B	↑	$x_{10} = 0.239 <$	$x_8 \cap x_{10} = 0.257$	$< 0.271 = x_8 + x_{10}$	C < A + B	↑
$x_3 = 0.095 <$	$x_3 \cap x_8 = 0.151$	$> 0.127 = x_3 + x_8$	C > A + B	↑↑	$x_{10} = 0.239 <$	$x_9 \cap x_{10} = 0.294$	$< 0.301 = x_9 + x_{10}$	C < A + B	↑
$x_3 = 0.095 <$	$x_3 \cap x_9 = 0.215$	$> 0.157 = x_3 + x_9$	C > A + B	↑↑					

Note: The symbol '∩' denotes the intersection between A and B. "↑" means that x_1 and x_2 are mutually enhanced, and "↑↑" means that x_1 and x_2 are non-linearly enhanced. The numbers in the table are q statistics.

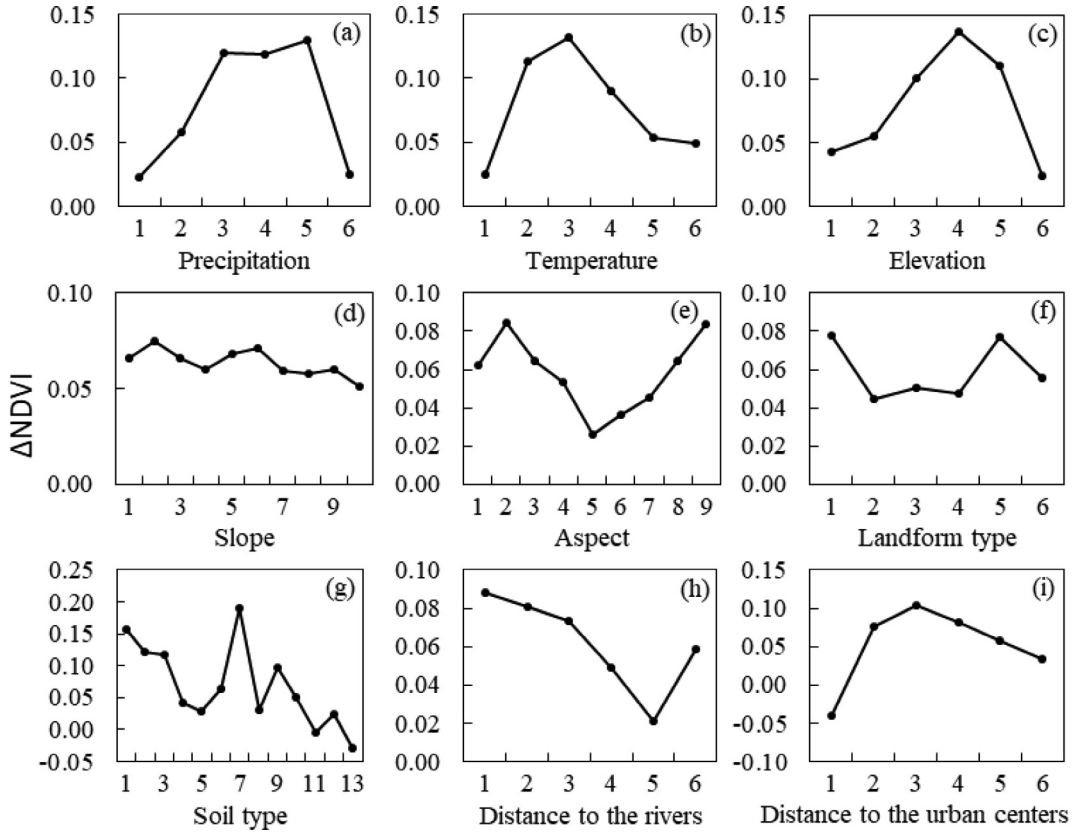

Fig. 6. Variations in the influence of factors with their levels.

magnitude of 0.025 at level 6 (509–675 mm). Temperature showed similar characteristics as precipitation (Fig. 6b). As elevation increased, the rate of NDVI increase first kept rising and reached the peak when the elevation is below 2791 m, and then decreased (Fig. 6c). A certain degree of elevation increase will not have negative influences on vegetation growth, but if the increase exceeds a critical value, the areas with extremely high elevation were often characterized by low temperature stress, large terrain fluctuations, poor soil quality and other harsh conditions which are not suitable for vegetation growth any more. The negative influence of high elevation on vegetation growth is particularly evident in Southwest China (Xiong et al., 2019). Compared to precipitation whose influence fluctuated largely, the impact of slope fluctuated slightly, which indicated that slope influenced NDVI in a nearly linear way (Fig. 6d). NDVI increasing rate at the first 6 levels (0–8.13°) is slightly larger than that at the last 4 levels (8.13°–27.58°), indicating that even terrains are more favorable for vegetation growth. Overall, NDVI increase on the shady and semi-shady slopes (North Slope) were greater than that on the sunny and semi-sunny slopes (South Slope) (Fig. 6e). The shady and semi-shady slopes with weaker evaporation and greater water retention capacity is better for vegetation growth than sunny and semi-sunny slopes (Zhu et al., 2016a), especially in arid areas. As the distance to the rivers increased, the magnitude of NDVI increase descended to the bottom of 0.02 at level 5 (30–50 km), and then increased a little to 0.06 when the distance to the rivers increased more. The distance of < 3 km to the urban centers led a decrease of 0.04 in NDVI, and NDVI started to increase with the increase of distance and reached the peak of 0.10 at level 3 (8–15 km), after which the magnitude of NDVI increase began to decrease.

Different types of land use conversion had different influence on NDVI variations (Table 6). From 2000 to 2015, most types of land use conversions had led to an increase in NDVI. Land use conversions, such as from unused lands to croplands, from grasslands to croplands and from forests to croplands, had caused the largest increasing magnitude of NDVI. There were only 7 types of land use conversion leading to a decrease in NDVI, of which the most prominent type was the conversion from cropland to construction land decreased by 0.075 with the largest area of 0.12%. We found that the *q* statistics for land use conversion from forests to unused lands are counter-intuitively positive, which indicated that such a type of conversion could cause an increase in NDVI. The reason for the unexpected results was that the area of this kind of conversion was only 1 km^2 (0.01% of the study area), and also had high error in detecting such conversion from forests to unused lands. The reason was the same for conversions from croplands to forests (0.01%), forests to grasslands (0.01%), forests to water areas (0.01%), water areas to grasslands (0.02%) and construction lands to unused lands (0.01%).

4. Discussion

4.1. Key natural drivers of NDVI change

Annual precipitation has the greatest influence on vegetation changes among natural drivers. This is consistent with the findings of previous studies that vegetation is more sensitive to precipitation than other natural factors in arid and semi-arid areas where water is a key limiting factor of vegetation growth (Chen and Ren, 2013; Liu et al., 2020). We found an interesting pattern that precipitation gradients dictate the relative importance of environmental and anthropogenic factors on vegetation in our study area. When precipitation is less (e.g., at level 1), the *q* statistics of land use conversion type and distance to the urban centers are much higher than other factors, indicating that NDVI change was mainly affected by human activities (Fig. 7). This is because precipitation is insufficient to meet water requirements of vegetation growth in these areas, while human activities could alleviate the limitations of precipitation by providing more water supply or transforming land use. When precipitation increased to level 2 and level

Table 6
Influences of land use conversion types on the magnitude of NDVI change.

2000\2015	Croplands	Forests	Grasslands	Water areas	Construction lands	Unused lands
Croplands	0.134 (18.68)	0.040 (0.01)	0.191 (0.15)	0.085 (0.02)	−0.075 (0.12)	−0.120 (0.07)
Forests	0.209 (0.07)	0.093 (6.34)	0.132 (0.01)	0.044 (0.01)		0.172 (0.01)
Grasslands	0.224 (0.68)		0.083 (22.50)	−0.006 (0.04)	0.021 (0.03)	0.044 (0.06)
Water areas	0.130 (0.03)		−0.003 (0.02)	0.079 (2.61)	−0.012 (0.01)	0.065 (0.02)
Construction lands					0.093 (1.65)	−0.416 (0.01)
Unused lands	0.259 (1.64)		0.107 (0.18)	−0.012 (0.10)	0.027 (0.22)	0.018 (44.74)

Note: The numbers in parentheses indicate the percentage of specific land use conversion to the total area (%). Blank cells indicate that this type did not occur in study area in study period.

3, the *q* statistics of natural factors such as temperature and slope increased significantly. This suggested that vegetation changes were mainly affected by both natural factors and human activities. When precipitation continued to increase to level 4 and level 5, the *q* statistics of mean annual temperature, elevation, landform type and soil type were significantly larger than other driving factors while the *q* statistic of land use conversion type was small, indicating that vegetation changes were mainly affected by natural factors. When precipitation reached level 6, land use conversion type became the key factor again. This indicated that environmental elements could not support vegetation growth much in the areas with harsh conditions such as extremely low temperatures, poor soil quality and steep slopes.

We found significant increase in NDVI in areas with hydromorphic soil, semi-leached soil and calcic soil. Hydromorphic soil is an important natural resource with high soil moisture and organic matter content. Semi-leached soil has a humus layer on the surface with rich calcium and magnesium, which has a strong fertilizer retention capacity. The semi-leached soil is important agricultural and forestry soil resources in semi-arid regions in China. Calcic soil has obvious humus accumulation in the surface layer and is rich in calcium (magnesium) carbonate. It is an important animal husbandry soil resource in China. The soil properties of hydromorphic soil, semi-leached soil and calcic soil were more favorable for vegetation growth than other soils, while glaciers and lakes and reservoirs had negative influences on vegetation changes.

4.2. Effects of human activities

Human activities indicated by land use change played an important role in vegetation change. Results from ecosystem models also support the key role of land use change in explaining vegetation change (Zhu et al., 2016b). We found most types of land use conversion occurred between 2000 and 2015 had positive influences on vegetation growth. The conversions from unused lands to croplands, unused lands to grasslands and grasslands to croplands increased NDVI by 0.259, 0.107, and 0.224, respectively, indicating that reasonable reclamation and regreening of unused lands and low-coverage grasslands had a positive effect on vegetation recovery during the study period. More intensive management of agriculture in our study area have resulted in an increase in NDVI of 0.134 in unchanged croplands. The direct evidence is the rapid increase in biomass and grain output from 886.45 million kilograms in 2000 to 1355 million kilograms in 2015 in Zhangye City which covers the main part of our study area. The measures to protect and manage forest resources, such as the construction of Qilian Mountain National Nature Reserve, has resulted in an increase in NDVI of 0.093 in unchanged forests. The implementation of several ecological protection projects such as the Grain for Green Project, Natural Forest Protection Project, and Three-north Forest Protection Project, caused the widespread land use conversions from croplands to grasslands and further led to an increase in NDVI of 0.191. Previous studies also support the effective role of ecological restoration project (e.g., afforestation, the grain for green policy) in promoting vegetation recovery (Piao et al., 2015; You et al., 2019). In contrast, some types of land use conversion had negative effects on vegetation growth. Farmland abandonment occurs when deteriorating environmental conditions are not suitable for cultivating, which results in the conversion from croplands to unused lands and the decrease in NDVI (−0.120). Rapid urbanization led to a large-scale shift from croplands to impervious surfaces. As can be seen from our research, the conversion from croplands to construction lands caused a decrease in NDVI (−0.075).

4.3. Non-linear effects and interactions of factors

Our research found that NDVI varied non-linearly with the levels of all influencing factors. With the increase in precipitation, the increase in NDVI driven by precipitation will decelerate. This is also supported by pervious study that there is a threshold for the response of vegetation changes to precipitation (Ukkola et al., 2016). The increase in NDVI driven by temperature reached the peak of 0.13 at level 3 (2.83–5.14 °C) and then began to decelerate, although NDVI increased

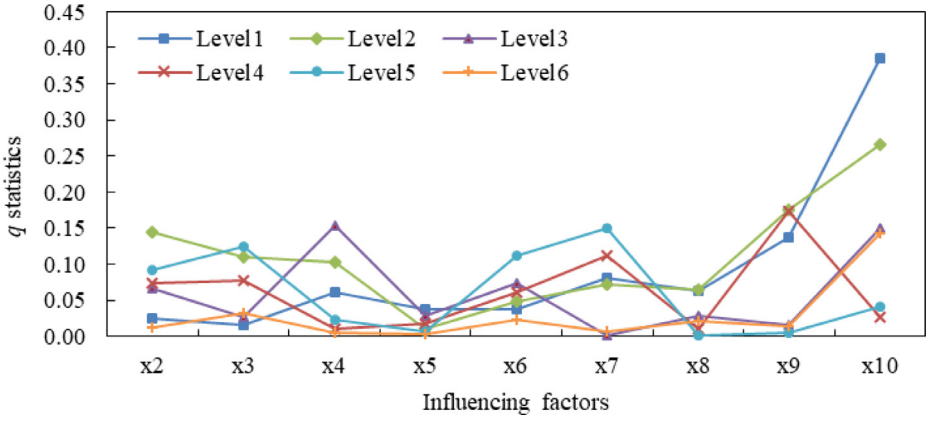

Fig. 7. *q* statistics of influencing factors of NDVI change along the gradient of mean annual precipitation.

consistently with temperature. When the temperature is at a much lower level, the physiological activities of vegetation is inhibited, and an appropriate temperature increase can promote photosynthesis, accelerate the release of soil nutrients and facilitate vegetation growth at this time (Zhou et al., 2001; Piao et al., 2006). Once beyond the tolerance range, extremely high temperature will increase transpiration and respiration, accelerate dry matter consumption and soil water loss, and weaken photosynthesis and nutrient transport, which is detrimental to vegetation growth (Zhang et al., 2015; Jiao et al., 2018). Distance to the rivers and to the urban centers were both related to NDVI change in a non-linear way. The river could support vegetation growth more at a closer distance within the 50 km limit, while once exceeded the role of the rivers weakened. Similarly, the distance to the urban centers also worked effectively in a certain range (15 km), a closer distance than the limit of distance to the rivers, beyond which the negative impact of urban construction on NDVI appeared to weaken.

The interactions between influencing factors often enhanced their effects on vegetation growth. Although elevation, temperature, distance to the urban centers, distance to the rivers, aspect, landforms and slope did not contribute ideally to NDVI change, their explanatory powers could be enhanced when interacting with others, especially mean annual precipitation and soil type. For example, the synergic effect of temperature and precipitation was stronger than the effect of each of a single factor ($x_2 \cap x_1 = 0.221 > x_2$). We can also see that human activities interacts with the natural conditions to influence vegetation changes. Natural factors, such as precipitation ($x_{10} \cap x_1 = 0.360 > x_{10}$), soil type ($x_{10} \cap x_7 = 0.327 > x_{10}$) and elevation ($x_{10} \cap x_3 = 0.311 > x_{10}$) often amplify the effect of human activities.

4.4. Effectiveness, limitations and future directions

Our research illustrated the effectiveness of the Geodetector method in identifying driving factors of vegetation in arid areas. Compared with traditional statistical methods and simulation models, it quantifies the non-linear responses of independent variables and their interactions to vegetation change, while avoiding the complexity of parameter settings. Vegetation will keep improving in most oasis areas of the middle reaches of the Heihe River Basin due to increasing precipitation and more developed irrigation system. However, the rapid urban expansion will lead to the loss of more lands with high vegetation productivity, causing a decrease in NDVI values in the future. This is implied by our findings that vegetation tends to significantly deteriorate in the areas close to the urban centers especially within 3 km. Our research has great implications for formulating land use policies and implementing measures to promote vegetation growth. More attention should be paid to green infrastructure construction such as parks during urban expansion. In the downstream areas measures should be taken to avoid salinization when improving irrigation facilities in agricultural areas and using water resources such as groundwater more effectively. Strict restrictions should be put to high-quality croplands, forests and grasslands so as to avoid losing high-quality land resources. There are still some shortcomings in our study. First, the influencing factors are not comprehensive. There is more and more evidence showing that the increase in CO_2 concentrations and the fertilization effect of nitrogen deposition are the possible driving factors for vegetation greening (Piao et al., 2015; Zhu et al., 2016b). Second, our research did not consider the spatial differentiation of the relationships between vegetation change and influencing factors. For example, precipitation has a significant and positive correlation with NDVI in areas of low-covered grassland, Gobi and deserts, while there is no or weak correlation between NDVI and precipitation in the oases because of abundant water resources from groundwater and irrigation (You et al., 2019). Further research should consider spatial and temporal heterogeneity of the relationships between vegetation change and its driving forces using pertinent methods of spatial statistics such as geographically weighted regression (GWR) and spatial panel data models.

5. Conclusions

We successfully derived the spatial and temporal patterns of vegetation changes in the middle reaches of the Heihe River Basin from 2000 to 2015, effectively quantified the effects of natural and anthropogenic factors on vegetation NDVI change using the Geodetector method. The vegetation conditions in the oases along the Heihe River and southern Qilian mountains were better than that in the northwest. Vegetation growth conditions across the study area improved from 2000 to 2015. The areas with significant improvement were mainly distributed along the Heihe River, and in the central and southern areas of our study area, while the areas with significant degradation were distributed sparsely around administrative centers. Both natural and anthropogenic factors influenced NDVI change, and the factors, land use conversion type, mean annual precipitation and soil type, caused the greatest influence. The influence of a single factor was often enhanced when it interacted with other factors. NDVI change often responded to the influencing factors in a non-linear way. Our research highlights that the Geodetector method is an effective way to disentangle the complicated driving factors of vegetation change, and our results is useful for projecting vegetation change under future environmental change.

CRediT authorship contribution statement

Lijun Zhu: Methodology, Software, Validation, Formal analysis, Investigation, Writing - original draft, Visualization. **Jijun Meng:** Conceptualization, Resources, Data curation, Writing - review & editing, Supervision, Project administration, Funding acquisition. **Likai Zhu:** Conceptualization, Methodology, Validation, Writing - review & editing, Funding acquisition.

Declaration of Competing Interest

The authors declare that they have no known competing financial interests or personal relationships that could have appeared to influence the work reported in this paper.

Acknowledgments

This work was supported by the National Natural Science Foundation of China (Grant No. 41871074), Shandong Provincial Natural Science Foundation, China (Grant No. ZR2019BD040), and the open fund of Ministry of Education Laboratory for Earth Surface Processes, Peking University.

References

A, D., Zhao, W., Qu, X., Jing, R., Xiong, K., 2016. Spatio-temporal variation of vegetation coverage and its response to climate change in North China plain in the last 33 years. Int. J. Appl. Earth Obs. Geoinf. 53, 103–117. https://doi.org/10.1016/j.jag.2016.08.008.

Casermeiro, M.A., Molina, J.A., Caravaca, M., Costa, J.H., Massanet, M., Moreno, P.S., 2004. Influence of scrubs on runoff and sediment loss in soils of Mediterranean climate. Catena 57, 91–107. https://doi.org/10.1016/S0341-8162(03)00160-7.

Chen, H., Ren, Z., 2013. Response of vegetation coverage to changes of precipitation and temperature in Chinese Mainland. Bull. Soil Water Conserv. 33 (2), 78–82. https://doi.org/10.13961/j.cnki.stbctb.2013.02.001.

Chen, W., Zhao, H., Li, J., Zhu, L., Zeng, J., 2020. Land use transitions and the associated impacts on ecosystem services in the Middle Reaches of the Yangtze River Economic Belt in China based on the geo-informatic Tupu method. Sci. Total Environ. 701, 134690. https://doi.org/10.1016/j.scitotenv.2019.134690.

Donohue, R.J., Roderick, M.L., McVicar, T.R., Farquhar, G.D., 2013. Impact of CO_2 fertilization on maximum foliage cover across the globe's warm, arid environments. Geophys. Res. Lett. 40 (12), 3031–3035. https://doi.org/10.1002/grl.50563.

Fu, J., Niu, J., Sivakumar, B., 2018. Prediction of vegetation anomalies over an inland river basin in north-western China. Hydrol. Process. 32 (12), 1814–1827. https://doi.org/10.1002/hyp.11626.

Gerten, D., Luo, Y., Le Maire, G., Parton, W.J., Keough, C., Weng, E., Beier, C., Ciais, P., Cramer, W., Dukes, J.S., Hanson, P.J., Knapp, A.A.K., Linder, S., Nepstad, D., Rustad, L., Sowerby, A., 2008. Modelled effects of precipitation on ecosystem carbon and water dynamics in different climatic zones. Glob. Change Biol. 14 (10), 2365–2379. https://doi.org/10.1111/j.1365-2486.2008.01651.x.

Gu, Z., Duan, X., Shi, Y., Li, Y., Pan, X., 2018. Spatiotemporal variation in vegetation coverage and its response to climatic factors in the Red River Basin, China. China. Ecol. Indic. 93, 54–64. https://doi.org/10.1016/j.ecolind.2018.04.033.

Hua, W., Chen, H., Zhou, L., Xie, Z., Qin, M., Li, X., Ma, H., Huang, Q., Sun, S., 2017. Observational quantification of climatic and human influences on vegetation greening in China. Remote Sens. 9 (5), 425. https://doi.org/10.3390/rs9050425.

Jiao, K., Gao, J., Wu, S., Hou, W., 2018. Research progress on the response processes of vegetation activity to climate change. Acta Ecol. Sin. 38, 2229–2238. https://doi.org/10.5846/stxb201702240305.

Li, F., Meng, J., Zhu, L., You, N., 2020. Spatial pattern and temporal trend of land degradation in the Heihe River Basin of China using local net primary production scaling. Land Degrad. Dev. 31 (4), 518–530. https://doi.org/10.1002/ldr.3468.

Liang, P., Yang, X., 2016. Landscape spatial patterns in the Maowusu (Mu Us) Sandy Land, northern China and their impact factors. Catena 145, 321–333. https://doi.org/10.1016/j.catena.2016.06.023.

Liu, C., Liu, B., Zhao, W., Zhu, Z., 2020. Temporal and spatial variability of water use efficiency of vegetation and its response to precipitation and temperature in Heihe River Basin. Acta Ecol. Sin. 40 (3), 1–12. https://doi.org/10.5846/stxb201810282323.

Liu, G., Liu, H., Yin, Y., 2013. Global patterns of NDVI-indicated vegetation extremes and their sensitivity to climate extremes. Environ. Res. Lett. 8 (2), 025009. https://doi.org/10.1088/1748-9326/8/2/025009.

Liu, L., Cao, W., Shao, Q., 2016. Change of ecological condition in the headwater of the Yangtze River before and after the implementation of the Ecological Conservation and Construction Project. J. Geo-Inf. Sci. 18, 1069–1076. https://doi.org/10.3724/SP.J.1047.2016.01069.

Liu, Y., Li, J., 2017. Geographic detection and optimizing decision of the differentiation mechanism of rural poverty in China. Acta Geogr. Sin. 72 (1), 161–173. https://doi.org/10.11821/dlxb201701013.

Los, S.O., 2013. Analysis of trends in fused AVHRR and MODIS NDVI data for 1982–2006: Indication for a CO_2 fertilization effect in global vegetation. Glob. Biogeochem. Cycle 27 (2), 318–330. https://doi.org/10.1002/gbc.20027.

Ma, Q., Jia, X., Wang, H., Li, Y., Li, S., 2019. Recent advances in driving mechanisms of climate and anthropogenic factors on vegetation change. J. Desert Res. 39 (6), 48–55. https://doi.org/10.7522/j.issn.1000-694X.2019.00004.

Mao, J., Shi, X., Thornton, P., Hoffman, F., Zhu, Z., Myneni, R., 2013. Global latitudinal-asymmetric vegetation growth trends and their driving mechanisms: 1982–2009. Remote Sens. 5 (3), 1484–1497. https://doi.org/10.3390/rs5031484.

Mueller, T., Dressler, G., Tucker, C., Pinzon, J., Leimgruber, P., Dubayah, R., Hurtt, G., Böhning-Gaese, K., Fagan, W., 2014. Human land-use practices lead to global long-term increases in photosynthetic capacity. Remote Sens. 6 (6), 5717–5731. https://doi.org/10.3390/rs6065717.

Oleson, K., Bonan, G., Feddema, J., Vertenstein, M., Kluzek, E., 2010. Technical description of an Urban Parameterization for the Community Land Model (CLMU). University Corporation for Atmospheric Research. https://doi.org/10.5065/D6K35RM9.

Pan, H., Huang, P., Xu, J., 2019. The spatial and temporal pattern evolution of vegetation NPP and its driving forces in middle-lower areas of the Min river based on geographical detector analyses. Acta Ecol. Sin. 39 (20), 7621–7631. https://doi.org/10.5846/stxb201809131971.

Peng, S., Piao, S., Shen, Z., Ciais, P., Sun, Z., Chen, S., Bacour, C., Peylin, P., Chen, A., 2013. Precipitation amount, seasonality and frequency regulate carbon cycling of a semi-arid grassland ecosystem in Inner Mongolia, China: a modeling analysis. Agric. For. Meteorol. 178, 46–55. https://doi.org/10.1016/j.agrformet.2013.02.002.

Peng, W., Kuang, T., Tao, S., 2019. Quantifying influences of natural factors on vegetation NDVI changes based on geographical detector in Sichuan, western China. J. Clean Prod. 233, 353–367. https://doi.org/10.1016/j.jclepro.2019.05.355.

Piao, S., Friedlingstein, P., Ciais, P., Zhou, L., Chen, A., 2006. Effect of climate and CO_2 changes on the greening of the Northern Hemisphere over the past two decades. Geophys. Res. Lett. 33 (23), L23402. https://doi.org/10.1029/2006GL028205.

Piao, S., Nan, H., Huntingford, C., Ciais, P., Friedlingstein, P., Sitch, S., Peng, S., Ahlström, A., Canadell, J.G., Cong, N., Levis, S., Levy, P.E., Liu, L., Lomas, M.R., Mao, J., Myneni, R.B., Peylin, P., Poulter, B., Shi, X., Yin, G., Viovy, N., Wang, T., Wang, X., Zaehle, S., Zeng, N., Zeng, Z., Chen, A., 2014. Evidence for a weakening relationship between interannual temperature variability and northern vegetation activity. Nat. Commun. 5, 5018. https://doi.org/10.1038/ncomms6018.

Piao, S., Wang, X., Ciais, P., Zhu, B., Wang, T., Liu, J., 2011. Changes in satellite-derived vegetation growth trend in temperate and boreal Eurasia from 1982 to 2006. Glob. Change Biol. 17 (10), 3228–3239. https://doi.org/10.1111/j.1365-2486.2011.02419.x.

Piao, S., Wang, X., Park, T., Chen, C., Lian, X., He, Y., Bjerke, J.W., Chen, A., Ciais, P., Tømmervik, H., Nemani, R.R., Myneni, R.B., 2019. Characteristics, drivers and feedbacks of global greening. Nat. Rev. Earth Environ. 1, 14–27. https://doi.org/10.1038/s43017-019-0001-x.

Piao, S., Yin, G., Tan, J., Cheng, L., Huang, M., Li, Y., Liu, R., Mao, J., Myneni, R.B., Peng, S., Poulter, B., Shi, X., Xiao, Z., Zeng, N., Zeng, Z., Wang, Y., 2015. Detection and attribution of vegetation greening trend in China over the last 30 years. Glob. Change Biol. 21 (4), 1601–1609. https://doi.org/10.1111/gcb.12795.

Qu, S., Wang, L., Lin, A., Yu, D., Yuan, M., Li, C., 2020. Distinguishing the impacts of climate change and anthropogenic factors on vegetation dynamics in the Yangtze River Basin, China. Ecol. Indic. 108, 105724. https://doi.org/10.1016/j.ecolind.2019.105724.

Reynolds, J.F., Stafford Smith, D.M., Lambin, E.F., Turner, B.L., Mortimore, M., Batterbury, S.P.J., Downing, T.E., Dowlatabadi, H., Fernandez, R.J., Herrick, J.E., Huber-Sannwald, E., Jiang, H., Leemans, R., Lynam, T., Maestre, F.T., Ayarza, M., Walker, B., 2007. Global desertification: Building a science for dryland development. Science 316 (5826), 847–851. https://doi.org/10.1126/science.1131634.

Sitch, S., Huntingford, C., Gedney, N., Levy, P.E., Lomas, M., Piao, S.L., Betts, R., Ciais, P., Cox, P., Friedlingstein, P., Jones, C.D., Prentice, I.C., Woodward, F.I., 2008. Evaluation of the terrestrial carbon cycle, future plant geography and climate-carbon cycle feedbacks using five Dynamic Global Vegetation Models (DGVMs). Glob. Change Biol. 14 (9), 2015–2039. https://doi.org/10.1111/j.1365-2486.2008.01626.x.

Ukkola, A., Prentice, I., Keenan, T., van Dijk, A., Viney, N., Myneni, R., Bi, J., 2016. Reduced streamflow in water-stressed climates consistent with CO_2 effects on vegetation. Nat. Clim. Change 6, 75–78. https://doi.org/10.1038/nclimate2831.

Wang, J., Li, X., Christakos, G., Liao, Y., Zhang, T., Gu, X., Zheng, X., 2010. Geographical detectors-based health risk assessment and its application in the neural tube defects study of the Heshun Region, China. Int. J. Geogr. Inf. Sci. 24, 107–127. https://doi.org/10.1080/13658810802443457.

Wang, J., Xu, C., 2017. Geodetector: principle and prospective. Acta Geogr. Sin. 72 (1), 116–134. https://doi.org/10.11821/dlxb201701010.

Wang, J., Yang, X., Zhang, Y., Wang, X., 2019. Correlation between NDVI and meteorological factors in Zhangye. Chin. Agric. Sci. Bull. 35, 85–90.

Wang, J., Zhang, T., Fu, B., 2016. A measure of spatial stratified heterogeneity. Ecol. Indic. 67, 250–256. https://doi.org/10.1016/j.ecolind.2016.02.052.

Wang, Y., Pan, J., 2019. Building ecological security patterns based on ecosystem services value reconstruction in an arid inland basin: A case study in Ganzhou District, NW China. J. Clean Prod. 241, 118337. https://doi.org/10.1016/j.jclepro.2019.118337.

Wessels, K.J., van den Bergh, F., Scholes, R.J., 2012. Limits to detectability of land degradation by trend analysis of vegetation index data. Remote Sens. Environ. 125, 10–22. https://doi.org/10.1016/j.rse.2012.06.022.

Wu, B., Ci, L.J., 2002. Landscape change and desertification development in the Mu Us Sandland, northern China. J. Arid. Environ. 50 (3), 429–444. https://doi.org/10.1006/jare.2001.0847.

Xiong, Q., He, Y., Li, T., Yu, L., 2019. Spatio temporal patterns of vegetation coverage and response to climatic and topographic factors in growth season in Southwest China. Res. Soil Water Conserv. 26, 259–266. https://doi.org/10.13869/j.cnki.rswc.2019.06.034.

Xu, X., 2018. China annual vegetation index (NDVI) spatial distribution dataset. Data Registration and Publishing System of Resource and Environment Science Data Center, Chinese Academy of Sciences (http://www.resdc.cn/DOI), 2018. DOI:10.12078/2018060601.

Yamori, W., Hikosaka, K., Way, D.A., 2014. Temperature response of photosynthesis in C_3, C_4, and CAM plants: temperature acclimation and temperature adaptation. Photosynth. Res. 119, 101–117. https://doi.org/10.1007/s11120-013-9874-6.

You, N., Meng, J., Sun, M., 2019. Spatio-temporal change of NDVI and its relationship with climate in the upper and middle reaches of Heihe River Basin from 2000 to 2015. Acta Sci. Natur. Univ. Pekinensis 55, 171–181. https://doi.org/10.13209/j.0479-8023.2018.075.

Yuan, L., Chen, X., Wang, X., Xiong, Z., Song, C., 2019. Spatial associations between NDVI and environmental factors in the Heihe River Basin. J. Geogr. Sci. 29 (9), 1548–1564. https://doi.org/10.1007/s11442-019-1676-0.

Zhang, D., Jia, Q., Xu, X., Yao, S., Chen, H., Hou, X., 2018. Contribution of ecological policies to vegetation restoration: A case study from Wuqi County in Shaanxi Province, China. Land Use Pol. 73, 400–411. https://doi.org/10.1016/j.landusepol.2018.02.020.

Zhang, J., Zang, C., 2019. Spatial and temporal variability characteristics and driving mechanisms of land use in the southeastern River Basin from 1990 to 2015. Acta Ecol. Sin. 39 (24), 9339–9350. https://doi.org/10.5846/stxb201810102187.

Zhang, J., Zheng, H., Zhu, L., Cui, Y., Zhang, X., Ye, L., 2017. Multi-dimensional changes of vegetation NDVI and its response to climate in Western Henan Mountains. Geogr. Res. 36 (4), 765–778. https://doi.org/10.11821/dlyj201704014.

Zhang, K., Kimball, J.S., Nemani, R.R., Running, S.W., Hong, Y., Gourley, J.J., Yu, Z., 2015. Vegetation greening and climate change promote multidecadal rises of global land evapotranspiration. Sci Rep 5, 15956. https://doi.org/10.1038/srep15956.

Zhou, L., Tucker, C.J., Kaufmann, R.K., Slayback, D., Shabanov, N.V., Myneni, R.B., 2001. Variations in northern vegetation activity inferred from satellite data of vegetation index during 1981 to 1999. J. Geophys. Res. 106 (17), 20069–20083. https://doi.org/10.1029/2000JD000115.

Zhu, Y., Wang, X., Wang, X., Deng, M., 2016a. Effect of slope aspect on the functional diversity of grass communities in the Loess Plateau. Acta Ecol. Sin. 36 (21), 6823–6833. https://doi.org/10.5846/stxb201505010900.

Zhu, Z., Piao, S., Myneni, R.B., Huang, M., Zeng, Z., Canadell, J.G., Ciais, P., Sitch, S., Friedlingstein, P., Arneth, A., Cao, C., Cheng, L., Kato, E., Koven, C., Li, Y., Lian, X., Liu, Y., Liu, R., Mao, J., Pan, Y., Peng, S., Peñuelas, J., Poulter, B., Pugh, T.A.M., Stocker, B.D., Viovy, N., Wang, X., Wang, Y., Xiao, Z., Yang, H., Zaehle, S., Zeng, N., 2016b. Greening of the earth and its drivers. Nat. Clim. Change 6, 791–795. https://doi.org/10.1038/nclimate3004.